

1 **The human  $\alpha$ -defensin-derived peptide HD5(1-9) inhibits cellular attachment and**  
2 **entry of human cytomegalovirus.**

3 **Rebecca Böffert<sup>1</sup>, Ramona Businger<sup>1</sup>, Hannes Preiß<sup>2</sup>, Dirk Ehmman<sup>3</sup>, Vincent**  
4 **Truffault<sup>4</sup>, Claudia Simon<sup>1</sup>, Natalia Ruetalo<sup>1</sup>, Klaus Hamprecht<sup>1</sup>, Patrick Müller<sup>2,5</sup>,**  
5 **Jan Wehkamp<sup>3</sup>, Michael Schindler<sup>1\*</sup>**

6

7 <sup>1</sup> Institute for Medical Virology and Epidemiology of Viral Diseases, University Hospital  
8 Tübingen, Tübingen, Germany

9 <sup>2</sup> Friedrich Miescher Laboratory of the Max Planck Society, Tübingen, Germany

10 <sup>3</sup> Department for Internal Medicine I, University Hospital Tübingen, Germany

11 <sup>4</sup> Max Planck Institute for Developmental Biology, Tübingen, Germany

12 <sup>5</sup> Translational Oncology Division, University Hospital Tübingen, Germany

13

14

15

16

17

18 \*Correspondence should be addressed to:

19 Michael Schindler, [michael.schindler@med.uni-tuebingen.de](mailto:michael.schindler@med.uni-tuebingen.de)

20

21

22 Running title: Defensin-derived peptides inhibit HCMV

23

24

25 **ABSTRACT**

26 Human cytomegalovirus (HCMV) infection causes severe illness in newborns and  
27 immunocompromised patients. Since treatment options are limited there is an unmet  
28 need for new therapeutic approaches. Defensins are cationic peptides, produced by  
29 various human tissues, which serve as antimicrobial effectors of the immune system.  
30 Furthermore, some defensins are proteolytically cleaved, resulting in the generation of  
31 smaller fragments with increased activity. Together, this led us to hypothesize that  
32 defensin-derived peptides are natural human inhibitors of virus infection with low toxicity.  
33 We screened several human defensin HNP4- and HD5-derived peptides and found  
34 HD5(1-9) to be antiviral without toxicity at high concentrations. HD5(1-9) inhibited HCMV  
35 cellular attachment and thereby entry and was active against primary as well as a  
36 multiresistant HCMV isolate. Moreover, cysteine and arginine residues were identified to  
37 mediate the antiviral activity of HD5(1-9). Altogether, defensin-derived peptides, in  
38 particular HD5(1-9), qualify as promising candidates for further development as a novel  
39 class of HCMV entry inhibitors.

40  
41  
42  
43  
44  
45  
46  
47  
48

49 **AUTHOR SUMMARY**

50 Defensins are peptides produced by various human organs which take part in the  
51 natural defense against pathogens. Recently, it has been shown that defensins are  
52 further cleaved to smaller peptides that have high intrinsic anti-microbial activity. We  
53 here challenged the hypothesis that these peptides might have antiviral activity, and due  
54 to their presumably natural occurrence, low toxicity. Indeed, we found one peptide  
55 fragment that turned out to block the attachment of the human cytomegalovirus (HCMV)  
56 to cells. Furthermore, this peptide did not show toxicity in various cellular assays or  
57 impede the embryonic development of zebrafish at the concentrations used to block  
58 HCMV. This is important, since HCMV is one of the most important viral congenital  
59 infections. Altogether, our results hold promise for the development of a new class of  
60 antivirals against HCMV.

61

62

63

64

65

66

67

68

69

70

71

72

## 73 INTRODUCTION

74 Human cytomegalovirus (HCMV) is a  $\beta$ -herpesvirus with a high prevalence worldwide  
75 (1). Being non- or mildly pathogenic in immunocompetent individuals it causes severe  
76 disease in newborns, is the major pathogen of viral congenital infections and is a  
77 constant threat for immunocompromised patients, especially after organ transplantation  
78 (2). Established treatment strategies are based on the polymerase inhibitors Ganciclovir  
79 (GCV) and Foscarnet (PFA), but both frequently cause severe adverse-effects and may  
80 induce rapid drug-resistance (3). Additionally, the cytosine phosphonate inhibitor  
81 Cidofovir (CDV) used as second-line agent for drug resistant herpesvirus infections can  
82 induce multi-drug resistance leading to potentially lethal outcome (4). The introduction of  
83 the cytomegalovirus terminase inhibitor Letermovir inspired hope for novel alternative  
84 therapeutic regimens, which was dampened by the recent description of Letermovir  
85 resistance in multiple patients (3, 5). Altogether, there is a still unmet and urgent need  
86 for new approaches to treat human cytomegalovirus infection; especially in difficult to  
87 treat patients for instance organ and stem cell transplant recipients, pregnant women  
88 and their fetuses, or congenitally HCMV-infected newborns.

89 Defensins are anti-microbial peptides produced by all animal species (6, 7). They have a  
90 size of 16-50 aminoacids (aa), are amphipathic, rich in arginines and therefore have an  
91 overall positive charge. The secondary structure mainly consists of 3  $\beta$ -strands that are  
92 stabilized by cysteine-build disulfide bonds. Depending on the size, abundance and  
93 overall structure they are categorized in  $\alpha$ -,  $\beta$ - and  $\theta$ -defensins.  $\alpha$ -defensins are further  
94 subdivided in myeloid (HNP1-4) and enteric defensins (HD5 and HD6) (7, 8).

95 The antimicrobial activity of defensins is best characterized against bacteria (9).

96 Defensins act in a multi-functional manner: they can penetrate membranes and form

97 pores, and they interact with nucleic acids and glycosylated proteins (10-13).  
98 Furthermore it was shown that defensins are involved in the formation of anti-microbial  
99 NET-structures (14). While all these features contribute to the broad activity of  
100 defensins, they are restricted to certain defensin species and associated with the  
101 specific structural features and aa-motifs.

102 Although less studied, defensins also have antiviral activity (15, 16). For instance,  $\alpha$ -  
103 defensins inhibit herpes simplex virus-2 (HSV-2) by interacting directly with viral particles  
104 or cellular heparan sulfates (17, 18). The  $\alpha$ -defensins HNP1-3 interfere with HIV-1  
105 glycoprotein binding to CD4, and the same defensins induce aggregation of Influenza-A  
106 virus and papillomaviruses (19-21). These examples show that  $\alpha$ -defensins harbor  
107 antiviral activity against enveloped and non-enveloped viruses. However, the potential  
108 inhibition of HCMV by defensins has not been comprehensively studied thus far.

109 Recently it was shown that the enteric  $\alpha$ -defensin HD5, but not HD6, undergoes  
110 proteolytic cleavage by human duodenal fluid resulting in the generation of HD5-derived  
111 peptides with potentially increased antimicrobial activity (22). We hypothesized that  
112 HD5-derived peptides might similarly have superior antiviral activity with low toxicity, as  
113 these molecules might naturally occur in humans. Indeed, here we identified HD5(1-9)  
114 as an attachment inhibitor of HCMV to various human cells with no toxicity at the  
115 concentrations in which they exert antiviral activity. Hence, defensin-derived peptides,  
116 and in particular HD5(1-9), are promising candidates for further development as a novel  
117 class of antiviral drugs.

118

119

120

## 121 **RESULTS**

### 122 **Human $\alpha$ -defensins HNP4 and HD5 inhibit HCMV infection.**

123 We first aimed to assess the potential antiviral activity against HCMV of the  $\alpha$ -defensins  
124 HNP4 (Fig. 1A) and HD5 (Fig. 1B) as well as defensin-derived peptides, occurring  
125 during natural proteolytic cleavage in human duodenal fluid (22) (Fig. 1). In a first  
126 approach, to assess potential toxicity, antiviral activity, as well as dose-dependency, we  
127 tested the defensins at two concentrations, high (75  $\mu$ M) and low (7.5  $\mu$ M) (Fig. 2). We  
128 infected primary human foreskin fibroblasts (HFF) with an HCMV-GFP reporter virus  
129 (MOI = 0.5) and added the peptides simultaneously with the infectious virus to the cells.  
130 At 40 hours post infection (hpi), cells were fixed, stained with DAPI, and the infection  
131 rate was calculated by automated cell counting (Fig. 2A, % GFP+/DAPI+ cells). Both full-  
132 length  $\alpha$ -defensins, HNP4 and HD5, inhibited HCMV infection at 75 but not at 7.5  $\mu$ M.  
133 Similar activity was observed for the short fragments HD5(1-9), HD5(7-32) and to a  
134 lesser extent for HNP4(1-11). Two peptides, HD5(1-9mod) and HNP4(1-11mod), were  
135 modified to protect them from proteases and increase activity by using D-aminoacids  
136 and by adding an acetate moiety to the N- and an amide moiety to the C-terminus (Fig.  
137 1). These two defensin-fragments also blocked HCMV-infection at 75  $\mu$ M (Fig. 2A).  
138 To evaluate potential toxicity of the peptides, we incubated HFF cells for 40 hours with  
139 the respective peptides and measured viability via MTT (Fig. 2B). This revealed  
140 moderate impairment of viability upon incubation with high concentrations of HNP4(1-  
141 11), HNP4(1-11mod) and all HD5-fragments with the exception of HD5(1-9) and HD5(1-  
142 9mod). Hence, antiviral effects exerted by HNP4, HD5 as well as HD5(1-9) and the  
143 modified version are not due to potential toxic effects of these peptides that would impair  
144 cellular viability. To further corroborate this finding, we visually inspected HCMV-infected

145 and peptide-treated cells by fluorescence microscopy and identified cells by DAPI-  
146 staining (Fig. 3). HCMV-infected cells express GFP as infection marker. Medium or  
147 solvent-treated cells show evenly distributed DAPI dots, resembling the nuclei of the  
148 cells within the monolayer. This pattern changes upon HCMV-infection, now showing  
149 several syncytia-like giant GFP+ cells, which is a cytopathic effect observed upon  
150 HCMV-infection (23). Addition of the antiviral active defensins, e.g. HNP4, HD5 or  
151 HD5(1-9), but not HD5(1-13) as an example of an inactive peptide, completely reverted  
152 this phenotype, blocked HCMV-infection as evident by the reduction of GFP+ cells and  
153 restored the homogenous morphology of the cellular monolayer, thus preventing HCMV-  
154 induced cytopathic effects (Fig. 3). In conclusion, we identified HNP4, HD5 as well as  
155 the HD5-derived peptide HD5(1-9) as natural human peptide inhibitors of HCMV.

156

### 157 **Cytotoxic potential exerted by $\alpha$ -defensin-derived peptides.**

158 Our initial assessment of peptide toxicity was after 40 hours of incubation by MTT,  
159 hence measuring mitochondrial activity of NADH/NADPH (24). To more carefully  
160 evaluate potential toxic effects of our  $\alpha$ -defensin peptides, we decided to use  
161 xCELLigence real-time monitoring of cellular viability (25). This system continuously  
162 measures the electrical impedance of single microtiter-plate wells. Conceivably, upon  
163 cell growth, impedance increases, whereas growth arrest or cellular detachment due to  
164 dying cells result in a drop of impedance. We further decided to test our collection of  
165 peptides not only on HFF, but also on ARPE-19 as a model cell line for epithelial cells  
166 and differentiated THP-1 or primary macrophages to model myeloid cells. All of these  
167 cells represent important HCMV target cell types *in vivo* (26, 27). Based on their ability  
168 to inhibit HCMV-infection at 75  $\mu$ M (Fig. 2A), we analyzed HNP4, HNP4(1-11), HNP4(1-

169 11mod), HD5, HD5(1-9), HD5(1-9mod) and HD5(7-32) (Fig. 4). Cells were first allowed  
170 to adhere. 24 hours post seeding we added the peptides at the concentrations indicated,  
171 and impedance was measured every 30 minutes. As expected, all effects observed were  
172 dose-dependent. HNP4 started to inhibit growth of all cell types at concentrations of 10  
173  $\mu\text{M}$  and was clearly cytotoxic at higher concentrations. HNP4(1-11) was only toxic when  
174 used above 75  $\mu\text{M}$  in HFF and ARPE-19 cells and non-toxic in primary macrophages.  
175 HNP4(1-11mod) induced cell death in all cell types starting at around 37.5  $\mu\text{M}$ . Similarly,  
176 HD5 showed high cytotoxic potential and already affected growth of for instance primary  
177 macrophages at 2-5  $\mu\text{M}$ . In strict contrast, HD5(1-9) was not cytotoxic for any of the cell  
178 types tested and only slightly affected growth of HFF and ARPE-19 at 150  $\mu\text{M}$  (Fig. 4).  
179 HD5(1-9mod) clearly reduced cell viability from 18.75  $\mu\text{M}$  on, whereas the longer  
180 peptide HD5(7-32) only showed cytotoxicity at very high concentrations. In sum, of all  
181 defensin peptides tested, only HD5(1-9) did not impair viability of the three different cell  
182 types over prolonged incubation.

183

#### 184 **Dose-dependent inhibition of HCMV-infection by $\alpha$ -defensin-derived peptides.**

185 Next, we analyzed the anti-HCMV activity of the selected candidate peptides on the  
186 three different cell lines in a dose-dependent manner. This allows calculating the  
187 inhibitory concentration 50 (IC<sub>50</sub>), i.e. the drug-concentration at which half-maximal  
188 antiviral activity is achieved. Again, cells were infected with HCMV at an MOI of 0.5 and  
189 the peptides were added together with the virus inoculum. 40 hours later cells were fixed  
190 and stained with DAPI and the viral immediate early (IE1/2) protein. Then infection rate  
191 was quantified by automated fluorescence microscopy (Fig. 5). In agreement with our  
192 previous data (Fig. 2A), all defensins inhibited HCMV infection in a dose-dependent



193 manner with only slight differences among the cell lines tested. However, since HNP4,  
194 HNP4(1-11mod), HD5 and HD5(1-9mod) also affected cell viability in our xCELLigence  
195 measurements (Fig. 4), these results have to be interpreted very carefully. Overall, as  
196 before, only HD5(1-9) showed antiviral activity at medium (50  $\mu$ M) to high concentrations  
197 (100  $\mu$ M) without cytotoxic effects (Fig.4 and Fig. 5). This is even more evident by  
198 looking at the CC50 (i.e. the drug-concentration at which half-maximal cytotoxic activity  
199 is observed) and IC50 values calculated from the data obtained from ARPE-19 cells as  
200 an example (Fig. 6). CC50 (Fig. 6A) and IC50 (Fig. 6B) values of HNP4, HNP4(1-11)  
201 and HD5 were highly similar, indicating that these peptides do not exert specific antiviral  
202 activity. HNP4(1-11mod) and HD5(7-32) are about two- to three-fold less toxic than  
203 antiviral, and HD5(1-9mod) was antiviral with an IC50 of  $\sim$ 14  $\mu$ M and clearly cytotoxic  
204 with a CC50 of  $\sim$ 57  $\mu$ M. Finally, HD5(1-9) had an IC50 of  $\sim$ 40  $\mu$ M and CC50 > 150  $\mu$ M  
205 indicating that this HD5-derived peptide fragment exerts specific antiviral activity against  
206 HCMV.

207

#### 208 **Effect of HD5(1-9) on embryonic development.**

209 As a first test of HD5(1-9) toxicity *in vivo*, as well as to elucidate potential effects of the  
210 peptide on embryonic development, experiments with zebrafish embryos were  
211 performed (28). Embryos were treated with HD5(1-9) at concentrations of 25  $\mu$ M, 75  $\mu$ M,  
212 125  $\mu$ M and 250  $\mu$ M starting at 6-7 hours post fertilization (hpf), which is the time point  
213 recommended by pharmaceutical company-utilized assays to assess toxic effects of  
214 compounds on early embryonic development (29). Phenotypes were analyzed at 13, 24  
215 and 48 hpf (Fig. 7). At the highest peptide concentration of 250  $\mu$ M, half of the embryos  
216 had died by 13 hpf, indicating that excess of HD5(1-9) can affect embryonic

217 development. Impaired development at 250  $\mu$ M peptide exposure was also evident over  
218 the whole observation period, leading to the death of 11 embryos and 4 embryos having  
219 severe developmental delays by 48 hpf (compare Fig. 7B, 7C and examples in Fig. 7D).  
220 Reduction of the peptide concentration to 125  $\mu$ M reduced the negative effects on  
221 embryonic development, with approximately half of the embryos having no alterations  
222 (Fig. 7C and 7D). Furthermore, all embryos treated with 25  $\mu$ M or 75  $\mu$ M of HD5(1-9)  
223 developed normally, except for one embryo that had died by 13 hpf due to unknown  
224 reasons (Fig. 7). Altogether, HD5(1-9) concentrations of 25  $\mu$ M to 75  $\mu$ M, which are  
225 higher than the IC<sub>50</sub> of ~40  $\mu$ M, do not affect zebrafish embryonic development or show  
226 toxicity *in vivo*.

227

#### 228 **HD5(1-9) inhibits multiresistant, primary HCMV isolates.**

229 HCMV TB40/E is a lab-adapted strain that might differ from primary HCMV isolates in  
230 terms of cellular tropism, infectivity or cytopathic properties. We hence tested whether  
231 HD5(1-9) is also active against primary HCMV isolates from different compartments of  
232 patients including amniotic fluid, breast milk and leukocytes (Fig. 8). Of note, the  
233 leukocyte isolate from a stem cell transplant recipient is genotypically (mutations UL97  
234 L595S, UL54 V715M) and phenotypically resistant against GCV (IC<sub>50</sub> > 30  $\mu$ M), PFA  
235 (IC<sub>50</sub> = 795  $\mu$ M), and CDV (IC<sub>50</sub> = 1.8  $\mu$ M) (4), while both isolates from amniotic fluid  
236 and breast milk were therapy-naive. We infected HFF cells at MOIs of 0.2 and 0.1 in the  
237 presence of increasing amounts of HD5(1-9). Similar to our previous results, HD5(1-9)  
238 inhibited HCMV infection efficiently at a concentration of 100  $\mu$ M in HFF. Importantly, not  
239 only infection with the lab-adapted TB40/E strain was blocked, but also infection with the

240 primary isolates was sensitive towards inhibition by HD5(1-9). Hence, HD5(1-9) is a  
241 peptide inhibitor active against primary as well as multiresistant HCMV strains.

242

### 243 **Structure-activity relationship of HD5(1-9) and HD5(1-13).**

244 In order to identify relevant amino acids regarding antiviral activity, HD5-derived  
245 peptides were designed. Arginine (Arg) residues were suggested to participate in HD5-  
246 membrane interactions, and hence HD5-mediated antimicrobial effects (30).  
247 Furthermore, Cysteine (Cys) at positions three and five are involved in forming disulfide  
248 bridges in the context of the full length protein and contribute to the biological activity of  
249 defensins (7, 16, 31). Therefore, we ordered three HD5(1-9) modified peptides: HD5(1-  
250 9)[R>A], where two Arg residues were mutated to alanine (Ala); HD5(1-9)[C>S] where  
251 both Cys were mutated to serine (Ser) and HD5(1-9)[C3S; C5R] where Cys3 was  
252 mutated to Ser and Cys5 to Arg. The latter one was done to test the effect of a  
253 membrane-interaction promoting additional Arg instead of a Cys (compare with HD5(1-  
254 9) peptide structure depicted in Fig.9A).

255 As before, HD5(1-9) inhibited HCMV at concentrations above 50  $\mu$ M when infecting  
256 HFF. In contrast, all of the modifications introduced abrogated the antiviral activity of  
257 HD5(1-9) (Fig. 9B). In conclusion, Cys as well as Arg residues within HD5(1-9) are  
258 important for the full antiviral activity of the peptide.

259 In our initial screen HD5(1-9) showed antiviral activity, whereas the four amino acid  
260 longer version HD5(1-13) was inactive (Fig. 2A). The peptide HD5(1-9) was predicted to  
261 be flexible and extended in solution (Fig. 9A), which was also confirmed by NMR  
262 spectroscopy. In contrast, algorithms to predict peptide structures (PEP-FOLD3, (32))  
263 show that HD5(1-13) is likely to adopt a “close” conformation, which might be stabilized

264 by the formation of a disulfide bond between Cys5 and Cys10 (Fig. 9C and D). This  
265 close conformation could explain the difference in activity between the peptides. To  
266 challenge this hypothesis, we designed and ordered another peptide HD5(1-13)[C10S],  
267 with the goal of opening the peptide conformation by disrupting a potential disulfide  
268 bridge formation involving Cys10. In keeping with previous results, HD5(1-13) did not  
269 inhibit HCMV infection (Fig. 9E). In contrast, HD5(1-13)[C10S] showed a gain-of-function  
270 phenotype and blocked HCMV infection at 75  $\mu$ M and 100  $\mu$ M.

271 Together, the data demonstrates that the antiviral activity of HD5-derived peptides is  
272 specific and can be enhanced by distinct amino acid modifications.

273

#### 274 **HD5(1-9) interferes with HCMV attachment and entry.**

275 In our infection assays, GFP controlled by the UL16 promoter or immunostaining of the  
276 HCMV IE1/2 antigen are markers for early viral gene expression, before *de novo* viral  
277 genome replication. We hence hypothesize that HD5(1-9) blocks an early event in the  
278 HCMV life cycle. We first set up an experiment to elucidate if HD5(1-9) acts directly on  
279 viral particles or exerts its antiviral activity on a cellular basis. For this, we pre-incubated  
280 virus stocks used for infection in small volumes for 1 h at 37 °C with the indicated  
281 concentrations of the peptide and added the mixture then to HFF, or performed the  
282 experiment as before, i.e. adding virus and peptide simultaneously to the cells (Fig.  
283 10A). In one condition, to assess if concentrated peptide is sufficient to neutralize  
284 infectivity of viral particles, HCMV stock and peptide were pre-incubated at 100  $\mu$ M of  
285 HD5(1-9). The mixture was then diluted 10-fold upon addition to the cells, resulting in a  
286 final concentration of 10  $\mu$ M HD5(1-9) during infection. However, neither pre-incubation  
287 of the peptide with virus stocks, nor incubation of virus in concentrated peptide solution

288 increased antiviral activity (Fig. 10A). These results suggest that HD5(1-9) exerts its  
289 antiviral activity not on assembled viral particles, but in the context of the cellular  
290 infection process.

291 We next used time-of-addition assays to investigate whether HD5(1-9) inhibits a pre- or  
292 post-entry step of HCMV infection. For this, we added HD5(1-9) either (i) three hours  
293 before infection, (ii) with the virus inoculum or (iii) three hours post-infection to the cells  
294 (Fig 10B). Of note, when HD5(1-9) was added to the cells three hours before infection,  
295 its activity was markedly increased. To the contrary, when added three hours post-  
296 infection, the peptide was nearly inactive in blocking HCMV-infection, even at a high  
297 concentration of 100  $\mu$ M (Fig 10C). This indicates that the antiviral activity of HD5(1-9) is  
298 attributable to an inhibition of HCMV cellular attachment or entry.

299 To directly assess, if HD5(1-9) blocks attachment of HCMV particles or entry of cell  
300 surface bound viruses, we employed a dual-fluorescently labeled virus (33). This allows  
301 to discriminate enveloped surface bound viruses (GFP+/mCherry+), from particles  
302 having lost their mCherry-labeled envelope during entry now appearing GFP+ only. We  
303 infected HFF cells at an MOI of 2 and added HD5(1-9) either during infection or 3 h later.  
304 Then cells were fixed, stained with Hoechst33342 and the amount of cell surface bound  
305 (GFP+/mCherry+) as well as penetrated viral particles (GFP+) quantified by  
306 fluorescence microscopy (Fig. 11). Upon addition of HD5(1-9), but not the inactive  
307 mutated peptide HD5(1-9)[R>A], the number of total cell surface bound particles was  
308 strongly reduced (quantitative analysis in Fig. 11A and representative images compare  
309 Fig. 11B). In contrast, when the same assay was performed with peptide added 3 h post  
310 infection, HD5(1-9) did not have an inhibitory effect on the amount of cell surface bound

311 or cell penetrated particles, which is overall consistent with an inhibition of HCMV  
312 attachment by HD5(1-9).

313

## 314 **DISCUSSION**

315 We here identified a natural human  $\alpha$ -defensin HD5-derived peptide as attachment  
316 inhibitor of HCMV. HD5(1-9) was non-toxic up to concentrations of 150  $\mu$ M for diverse  
317 cell types and showed antiviral activity starting at concentrations higher than 50  $\mu$ M in  
318 HFF cells and 25  $\mu$ M in ARPE-19 with an IC<sub>50</sub> of  $\sim$ 40  $\mu$ M in ARPE-19 (Fig. 6). This  
319 antiviral effect was highly specific, since we could disrupt the activity of the peptide by  
320 mutating Cys3 and Cys5 as well as Arg6 and Arg9 (Fig. 9). In addition, other HD5-  
321 derived peptides did not show antiviral activity or were clearly cytotoxic when used at  
322 similar concentrations. Of note, we could also demonstrate a gain-of-function for the four  
323 amino acid longer version HD5(1-13) by mutation of Cys10 to Ser. This could be  
324 explained by the opening of the close conformation predicted for HD5(1-13), since the  
325 substitution of Cys10 to Ser would impair the formation of a disulfide bridge, which could  
326 maintain the structure closed. This confers antiviral activity to HD5(1-13) blocking HCMV  
327 infection at 75  $\mu$ M and above (Fig. 9). Moreover, this demonstrates that it is possible to  
328 improve antiviral activity of the small HD5-derived peptides *per se* by single amino acid  
329 exchanges. Hence, it is tempting to speculate that the activity of HD5(1-9) could be  
330 improved for instance by shortening of the N-terminus or changing glycine at position  
331 eight into arginine to further increase the positive charge of the peptide. However, such  
332 modifications have to be introduced with caution. HD5(1-9mod), composed of D-amino  
333 acids and equipped with an N-terminal acetate and a C-terminal amide-group to render it

334 more stable and prevent degradation, showed high toxicity over prolonged incubation on  
335 various cell types (Fig. 4).

336 In this context, it has to be noted that toxicity is a critical parameter when determining  
337 the antiviral activity of drug candidates. Viruses are obligatory intracellular pathogens  
338 that use the cellular machinery for propagation. Hence, any compound-induced  
339 impairment of viability could negatively impact viral replication. We performed various  
340 independent assays to determine the potential cytotoxicity of our peptide candidates: (i)  
341 MTT assays measuring the metabolic activity of cells; (ii) adherence and growth by  
342 monitoring the electrical impedance of cells when they are cultured as monolayers on  
343 plates; and (iii) peptide effects on embryonic development of zebrafish. Remarkably,  
344 while in MTT none of the peptides dramatically affected metabolic activity (Fig. 2B), only  
345 HD5(1-9) did not impair long-term growth and adherence of cells in high concentration  
346 (Fig. 4). In zebrafish embryonic development, we did not observe toxicity of HD5(1-9) at  
347 concentrations that were nearly twice as high as its IC<sub>50</sub> (Fig. 7).

348 Defensins have been described as antiviral effector molecules of various viruses with  
349 different potential modes of action (16, 34). Nevertheless, this is the first comprehensive  
350 report demonstrating antiviral activity of a defensin against HCMV and in particular of the  
351  $\alpha$ -defensin HD5-derived peptide HD5(1-9). Just recently, Ehmann and colleagues  
352 provided compelling evidence that defensins are cleaved by proteolytic processes and  
353 that the resulting peptides - including HD5(1-9) - have broad antimicrobial activity (22).  
354 Administration of HD5(1-9) via the oral route was well tolerated in mice and elicited  
355 microbiome-modulating activity *in vivo*. However, neither parenteral administration nor  
356 bioavailability of HD5(1-9) in blood and organs after oral consumption have been  
357 analyzed yet.

358 HCMV poses a serious threat for immunocompromised patients, for instance HIV-1-  
359 infected individuals or transplant recipients. Treatment with GCV is often problematic,  
360 since it has a high nephrotoxic potential and the resistance barrier is low. The terminase  
361 inhibitor Letemovir is a therapeutic alternative, but first resistance-conferring mutations  
362 have been described (3, 5). In this regard, the establishment and testing of new  
363 treatment options is necessary. Even though the HD5-derived peptides analyzed within  
364 our study are at a proof-of-principle stage and currently far from being used as antiviral  
365 drugs, their further development holds a variety of potentially attractive promises: (i) due  
366 to the small size of just nine amino acids HD5(1-9) is affordable and realistic to develop,  
367 even as peptide inhibitor; (ii) the mode of action is block of viral attachment to cells,  
368 thereby protecting them from infection; (iii) HD5(1-9) acts on a cellular target, minimizing  
369 the risk of resistance development; (iv) as attachment inhibitor, HD5(1-9) binds to the  
370 cell surface and hence does not have to penetrate cells; (v) HD5(1-9) has a broad  
371 antimicrobial activity and therefore might also protect from bacterial as well as other viral  
372 infections.

373 Altogether, we provide proof-of-concept for the use of  $\alpha$ -defensin HD5-derived peptides,  
374 in particular HD5(1-9), as potential entry inhibitors of lab-adapted, as well as primary and  
375 multiresistant human cytomegalovirus strains. The advantages associated with the use  
376 of defensin-derived peptides for the therapy of human viral diseases warrants their  
377 further in-depth analyses and preclinical development.

378

## 379 **MATERIAL AND METHODS**

380 **Cell culture.** Primary human macrophages (isolated from buffy coat of healthy blood  
381 donors, see details below), primary human foreskin fibroblasts (HFF; from ATCC



382 #SCRC-1041), ARPE-19 (from ATCC #CRL-2302), and THP-1 (from the NIH AIDS  
383 reagent program #9942) were cultured at 37 °C with 5% CO<sub>2</sub>. Primary human  
384 macrophages were prepared and differentiated as follows and maintained in  
385 macrophage-medium (RPMI supplemented with 4% human AB serum, 2 mM L-  
386 Glutamine, 100 µg/ml penicillin/streptomycin, 1 mM sodium pyruvate, 1x non-essential  
387 amino acids and 0.4x MEM vitamins). HFF and ARPE-19 were cultured in DMEM  
388 containing 5% FCS as well as 2 mM L-Glutamine and 100 µg/ml penicillin/streptomycin.  
389 THP-1 cells were maintained in RPMI containing 0.25 µg/ml puromycin supplemented  
390 with 10% FCS, 2 mM L-Glutamine and 100 µg/ml penicillin/streptomycin. For the  
391 respective experiments, THP-1 cells were differentiated with 30 ng/ml phorbol-myristate-  
392 acetate (PMA) for 24 h at 37 °C.

393 **Isolation and differentiation of primary human macrophages.** Macrophages were  
394 generated from buffy coats of healthy blood donors who gave informed consent for the  
395 use of blood-derived products for research purposes. We do not collect data concerning  
396 age, gender or ethnicity and comply with all relevant ethical regulations (IRB  
397 #507/2017BO1). All buffy coat donations were received in anonymous form and chosen  
398 randomly. PBMCs were isolated from buffy coats by biocoll density gradient  
399 centrifugation and differentiated 3 days by plastic adherence in macrophage-medium.  
400 After 3 days, non-adherent cells were removed by washing, and the macrophages were  
401 further differentiated 4 days with macrophage-medium.

402 **Infection assays and HCMV viral stocks.** For generating HCMV stocks HFF cells were  
403 infected with TB40-ΔUL16-eGFP essentially as described before (35). Infectious  
404 supernatant was harvested 5 to 7 dpi and subsequently cleared from cells and cellular  
405 debris by centrifuging 10 min at 3200 x g.

406 HFF and ARPE-19 were seeded with 10 000, macrophages with 20 000 and THP-1 with  
407 50 000 cells per well of a 96-well plate. Peptides and the virus were added  
408 simultaneously. The respective MOI is indicated in the figure legends. 40 hpi, the cells  
409 were fixed with 2% PFA (10 min at 37 °C, 20 min at room temperature or overnight at 4  
410 °C) and permeabilized with ice-cold 90 % methanol in H<sub>2</sub>O for 20 min at 4 °C. Cells were  
411 further stained for IE1/2 (mouse anti HCMV IE E13, Argene, 1:1000 dilution in PBS) and  
412 counterstained with goat-anti-mouse Alexa594 (Thermo, 1:2000 dilution in PBS)  
413 followed by DAPI. Images were taken with the Biotek Cytation 3 multiplate reader. The  
414 infection rate was calculated by the number of IE1/2-positive signals to the number of  
415 DAPI-positive cell nuclei.

416 **Screening of the peptide set for antiviral activity.** Peptides were solved in PBS or  
417 0.01% HAc. The full-length peptide HNP4 and its derivatives HNP4(1-11) and HNP4(1-  
418 11mod) as well as the full-length peptide HD5 and its derivatives HD5(1-9), HD5(1-  
419 9mod), HD5(1-13), HD5(1-28), HD5(7-32), HD5(10-27), HD5(10-32) and HD5(26-32)  
420 were obtained from EMC microcollections GmbH and tested for their antiviral activity  
421 against HCMV TB40/E- $\Delta$ UL16-eGFP on HFF at concentrations of 7.5  $\mu$ M and 75  $\mu$ M  
422 respectively. A MOI of 0.5 was used. For evaluation of infection, GFP was used as  
423 readout and images were taken with the Biotek Cytation 3 multiplate reader. The  
424 infection rate was calculated by the number of GFP-positive cells to the number of DAPI-  
425 positive cell nuclei.

426 **Screening of the peptide set for cytotoxicity: MTT assay.** The cell viability of HFF  
427 after treatment with the peptides HNP4, HNP4 (1-11), HNP4 (1-11mod), HD5, HD5 (1-  
428 9), HD5 (1 9mod), HD5 (1-13), HD5 (1-28), HD5 (7-32), HD5 (10-27), HD5 (10-32) and  
429 HD5 (26-32) was measured at different concentrations by standard MTT measurement

430 (24). For the screening tests 10 000 HFF were seeded in 96-well plates. The peptides  
431 were tested at concentrations of 7.5  $\mu$ M and 75  $\mu$ M. 40 h post treatment, the medium  
432 was changed to 90  $\mu$ l phenol red free medium, and MTT solution was added and  
433 incubated for 3 h. The medium was removed and the crystals were dissolved in 100  $\mu$ l  
434 0.04 M hydrochloric acid in isopropanol for 10 min. Absorption was measured in the  
435 Biotek Cytation 3 multiplate reader at 570 and 650 nm. For evaluation, the mean  
436 absorption value measured in empty wells was subtracted from all measured absorption  
437 values. To determine the absolute absorption the absorption values of the reference  
438 wavelength 650 nm were subtracted from the values at 570 nm. The relative absorption  
439 was determined by referring the corresponding value to the mean absorption of the HFF  
440 treated with 0.01% HAc. The experiment was performed three times and technical  
441 triplicates were used.

442 **Determination of CC50 for selected peptides: impedance measurement.** Analogous  
443 to the determination of IC50, the toxicity of the peptides HNP4, HNP4(1-11), HNP4(1-  
444 11mod), HD5, HD5(1-9), HD5(1-9mod) and HD5(7-32) was investigated in more detail  
445 by determining the peptide concentration at which 50 % of the cells show a cytotoxic  
446 effect (CC50). The xCELLigence system was used for this purpose. The principle is  
447 based on a measurement of the electrical impedance caused by adhesive cells on the  
448 bottom of a 96-well plate equipped with microelectrodes. Cell proliferation causes an  
449 increase in impedance due to partial isolation of the electrodes, while events leading to  
450 altered cell morphology or cell detachment lead to decreased impedance (25).

451 The experiments were performed with HFF, ARPE-19 and macrophages. 10 000 HFF or  
452 ARPE-19 or 20 000 macrophages per well were seeded. The plate was placed in the  
453 xCELLigence, and the impedance was measured at 37 °C and 5% CO<sub>2</sub> for 24 h every

454 30 min. The plate was then removed, and a media change and treatment with the  
455 peptides were performed. The peptide concentrations corresponded to a two-fold serial  
456 dilution from 150  $\mu$ M to 2.34  $\mu$ M. The positive control was 10% Triton-X. Afterwards, the  
457 impedance at the bottom of the 96-well plate was measured every 30 min for a further  
458 72 h. The calculation of the CC50 was done analogously to the calculation of the IC50 in  
459 GraphPad Prism 7.0.

460 **Determination of IC50 for selected peptides.** IC50 values were measured for the  
461 peptides HNP4, HNP4(1-11), HNP4(1-11mod), HD5, HD5(1-9), HD5(1-9mod) and  
462 HD5(7-32). A two-fold serial dilution of the peptides was done from 100  $\mu$ M to 1.56  $\mu$ M.  
463 The experiments were performed on HFF and ARPE-19 cells with an MOI of 0.5, on  
464 THP-1 cells with an MOI of 10 and on primary macrophages with an MOI of 70. The  
465 IC50 was calculated in GraphPad Prism 7.0. For this purpose, a dose-response curve  
466 was created with the values of the relative infection rate. The relative infection rate of  
467 untreated infected cells was the starting point of the curve, and for technical reason the  
468 value "0" was substituted in the logarithmic scale for  $10^{-10}$ .

469 **Experiments with zebrafish.** To test HD5(1-9) for toxicity and to assess its effect on  
470 embryonic development in zebrafish, embryos obtained from natural crosses of wildtype  
471 TE fish were used. After mating, embryos were incubated at 28°C until 6 hours post-  
472 fertilization (hpf). Triplicates of five embryos each were then placed in wells of a 96-well  
473 plate containing 200  $\mu$ l of different peptide concentrations. HD5(1-9) dissolved in PBS  
474 was diluted in normal embryo medium (250 mg/L Instant Ocean salt, 1 mg/L methylene  
475 blue in reverse osmosis water adjusted to pH 7 with NaHCO<sub>3</sub>) (36). The concentrations  
476 tested were 25  $\mu$ M, 75  $\mu$ M, 125  $\mu$ M and 250  $\mu$ M, and the concentration of PBS solvent  
477 was adjusted for each control group. At peptide concentrations of 75  $\mu$ M and above we

478 observed granulae in some wells, which could represent peptide accumulations. As a  
479 control, embryos were additionally incubated in 25 µg/ml cycloheximide (C4859, Sigma-  
480 Aldrich). After 13 hpf, 24 hpf and 48 hpf a microscopic phenotype analysis was  
481 performed. For each time point embryos were automatically imaged using an  
482 ACQUIFER Imaging Machine. For the phenotype analysis at 48 hpf, the larvae were  
483 manually dechorionated and anaesthetized with 2% tricaine methanesulfonate (A5040-  
484 25G, Sigma-Aldrich). Images were acquired on an Axio Zoom.V16 microscope (ZEISS).

485 **Infection assays with clinical isolates.** The antiviral activity of HD5(1-9) in  
486 concentrations from 1.56 µM to 100 µM against infection with clinical HCMV isolates  
487 was investigated on HFF. In addition to the laboratory-adapted strain TB40/E-ΔUL16-  
488 eGFP, which served as reference strain, a breast milk-derived strain, an amniotic fluid-  
489 isolated strain and a multidrug-resistant viral isolate from leukocytes of a recipient after  
490 the third stem cell transplantation were used. The therapy-naïve strain from cell free milk  
491 whey (H1241-2016) was derived from a mother of a preterm infant 10 weeks postpartum  
492 during end of viral reactivation. The amnion fluid derived virus strain (H2497-2011) was  
493 isolated following termination of pregnancy based on severe fetal brain damage  
494 (Preisetanz, S, Diploma thesis, University of Tuebingen, 2012). The multidrug resistant  
495 CMV isolate (H815-2006) is already described (4). This viral isolate showed the  
496 canonical UL97 mutation L595S and an UL54 mutation V715M, leading to drug  
497 resistance against GCV, IC<sub>50</sub> = 31.5 µM, and CDV, IC<sub>50</sub> = 795 µM. IC<sub>50</sub> value against  
498 PFA was 1.8 µM. All viral isolates were primarily HFF-adapted and propagated in vitro  
499 with at least 10 passages to get TCID values of cell free viral supernatants of 10<sup>5</sup> to  
500 10<sup>6</sup>/ml.

501 **Infection assays with derivatives of peptide fragments.** For structure-activity  
502 relationship HD5(1-9) derivatives with modified amino acids were ordered from JPT  
503 Peptide Technologies GmbH. Peptides were solved in PBS or 0.01% HAc at a  
504 concentration of 1 mM. The antiviral activity of HD5(1-9), HD5(1-9) [R6>A], HD5(1-9)  
505 [C>S], HD5(1-9) [C3S, C5R] and HD5(1-13) [C10S] was tested in concentrations from  
506 1.56  $\mu$ M to 100  $\mu$ M on HFF cells. All experiments were performed three times with an  
507 MOI of 0.2 using technical duplicates.

508 **NMR spectroscopy.** The unlabeled peptide HD5(1-9) (JPT Technologies) was  
509 dissolved in acetic acid 0.01% to a final concentration of 1mM. All NMR spectra required  
510 for chemical shift assignment were acquired on Bruker AVIII-600 spectrometer. All  
511 spectra were recorded at 298 K. The NMR data were processed using TopSpin 2.1  
512 (Bruker GmbH), and analyzed with Sparky 3.115 (37). In-Phase COSY was acquired  
513 with 4096 and 128 complex points in  $t_2$  and  $t_1$ , respectively, performing 16 scans per  
514 increment (38). The TOCSY experiment was recorded with 4096 ( $t_2$ ) x 256 ( $t_1$ ) complex  
515 points using 16 scans per increment and a relaxation delay of 1.5 s. The NOESY  
516 spectrum was acquired on Bruker AVIII-800 using 1024 ( $t_2$ ) x 172 ( $t_1$ ) complex points  
517 using 96 scans per increment and a relaxation delay of 1.5 s. The NOESY spectrum was  
518 recorded with a NOE mixing time of 80 ms and the TOCSY spectrum was recorded with  
519 a spin lock mixing time of 70 ms. The HMQC-COSY and HMBC spectrum were recorded  
520 at a resolution of 1024 ( $t_2$ ) x 172 ( $t_1$ ) complex points, with 256 scans per increment. The  
521  $^{13}$ C-HSQC was recorded at a resolution of 1024 ( $t_2$ ) x 128 ( $t_1$ ) complex points, using  
522 128 scans per increment.

523 **Preincubation assays.** To assess direct binding of HD5(1-9) to viral particles, the  
524 peptide was incubated for one hour at 37 °C with the virus in concentrations of 1.56  $\mu$ M

525 to 100  $\mu$ M and then given to HFF. As reference, the infection assay was performed at  
526 the same concentrations without preincubation. In one condition, peptide and virus were  
527 pre-incubated at a peptide concentration of 100  $\mu$ M in a volume of 10  $\mu$ l and diluted on  
528 the cells to a concentration of 10  $\mu$ M in 100  $\mu$ l volume. The experiment was performed  
529 three times with a MOI of 0.2 using technical duplicates.

530 **Time-of-addition assays.** (i) Peptide was pre-incubated with cells for 3 h at 37 °C  
531 before addition of the virus. (ii) Peptide and virus were added to HFF simultaneously or  
532 (iii) the peptide was added to the cells 3 h after the virus. In all conditions, incubation  
533 volumes and peptide concentrations were adjusted to achieve a range of peptide  
534 concentrations of 1.56  $\mu$ M to 100  $\mu$ M. This experiment was performed three times with a  
535 MOI of 0.2 using technical duplicates.

536 **Infection assays with a dual fluorescent virus.** In order to investigate the mode of  
537 action of HD5(1-9), an infection assay with the dual fluorescent virus TB40-BAC<sub>KL</sub>-  
538 UL32eGFP-UL100mCherry on HFF was performed (33). This is an endotheliotropic  
539 HCMV strain expressing pp150 (pUL32) fused to eGFP and gM (pUL100) fused to  
540 mCherry. This allows discriminating enveloped virus particles, which have the green  
541 capsid and the red envelope and thus appear yellow, from already penetrated virus  
542 particles which lost their red envelope and only show eGFP signal. 20 000 HFF were  
543 seeded in 8-well-chamber-slides (IBIDI). The cells were infected with an MOI of 2 and  
544 the peptides (HD5(1-9) and HD5(1-9)[R>A]) were added either simultaneously with the  
545 virus or 3 hpi at a final concentration of 100  $\mu$ M. After 6 h the cells were fixed and  
546 stained with 1  $\mu$ g/ml Hoechst33342 in PBS for 10 min at RT. After fixation and staining,  
547 the cells were washed three times with 200  $\mu$ l PBS each. Images were taken with the

548 Deltavision OMX (GE Healthcare) in confocal mode and virus particles were counted  
549 with Fiji (ImageJ).

550 **Software, analysis tools, and molecular modeling.** GraphPad Prism 7.0 was used for  
551 statistical analyses and generation of diagrams. The respective statistical test used is  
552 indicated in each figure legend. Other software used was Gen5 V2.09 (Biotek), Imaris  
553 and SoftWorx (GE Healthcare) for image acquisition and analyses. Electrical impedance  
554 was measured by xCELLigence (OLS) and analyzed by the RTCA (ACEA Biosciences)  
555 software. For de novo structure prediction the online PEP-FOLD3 predictor was used.  
556 Structural representations were prepared with PyMOL (The PyMOL Molecular Graphics  
557 System, Version 1.7.7.6 Schrödinger, LLC).

558 **Ethics statement.** Macrophages were generated from buffy coats of healthy blood  
559 donors who give written informed consent for the use of blood-derived products for  
560 research purposes (IRB# 507/2017BO1). We do not collect data concerning age, gender  
561 or ethnicity and comply with all relevant ethical regulations. All buffy coat donations are  
562 received in anonymous form and chosen randomly. Ethics board approval was not  
563 required for our work with zebrafish embryos. According to the Directive 2010/63/EU of  
564 the European Parliament and of the EU Council on the protection of animals used for  
565 scientific purposes, only experiments on freely feeding larvae (i.e. after day 5 of  
566 development) are considered “Research on Animals”. Therefore, this definition does not  
567 apply to our experiments, which focused on early embryonic development before day 5  
568 of development. In detail, we observed embryonic development until 48 hours post  
569 fertilization.

570

571



572 **Author contributions**

573 RBö, RBu, VT, CS, NR, PM and MS designed experiments. RBö, RBu, HP and VT  
574 performed experiments. RBö, RBu, HP, NR, PM and MS analyzed the data. DE, KH, JW  
575 and MS contributed reagents and analysis tools. MS wrote the manuscript, conceived  
576 the overall study and developed the manuscript to its final form. All authors contributed  
577 to manuscript editing, read and approved the final manuscript draft.

578

579 **Competing Interests**

580 The authors declare the following personal interest: RBö, RBu, DE, JW and MS filed a  
581 patent application for the use of  $\alpha$ -defensin-derived peptides, in particular HD5(1-9), as  
582 antiviral inhibitor of human cytomegalovirus. The patent is currently pending.

583

584 **Acknowledgements**

585 We are grateful to Christian Sinzger for providing HCMV constructs and giving helpful  
586 comments and suggestions. We would further like to thank Ulrich Lauer and his team for  
587 support with xCELLigence measurements and the team of the Transfusion Medicine at  
588 the University Hospital Tübingen (Taman Bakchoul) for providing buffy coats. This work  
589 was in part funded by basic research support given from the University Hospital  
590 Tübingen, Medical Faculty as well as an IZKF stipend to Rebecca Böffert.

591 **Data availability**

592 All data generated and analyzed during this study are included in this published  
593 manuscript. Further datasets supporting this study are available from the corresponding  
594 author upon request.

595

596 **References**

- 597
- 598 1. Cannon MJ, Schmid DS, Hyde TB. Review of cytomegalovirus seroprevalence  
599 and demographic characteristics associated with infection. *Reviews in medical virology*.  
600 2010;20(4):202-13.
  - 601 2. Griffiths P, Baraniak I, Reeves M. The pathogenesis of human cytomegalovirus.  
602 *The Journal of pathology*. 2015;235(2):288-97.
  - 603 3. Britt WJ, Prichard MN. New therapies for human cytomegalovirus infections.  
604 *Antiviral Res*. 2018;159:153-74.
  - 605 4. Göhring K, Wolf D, Bethge W, Mikeler E, Faul C, Vogel W, et al. Dynamics of  
606 coexisting HCMV-UL97 and UL54 drug-resistance associated mutations in patients after  
607 haematopoietic cell transplantation. *J Clin Virol*. 2013;57(1):43-9.
  - 608 5. Jung S, Michel M, Stamminger T, Michel D. Fast breakthrough of resistant  
609 cytomegalovirus during secondary letermovir prophylaxis in a hematopoietic stem cell  
610 transplant recipient. *BMC Infect Dis*. 2019;19(1):388.
  - 611 6. White SH, Wimley WC, Selsted ME. Structure, function, and membrane  
612 integration of defensins. *Current opinion in structural biology*. 1995;5(4):521-7.
  - 613 7. Shafee TM, Lay FT, Phan TK, Anderson MA, Hulett MD. Convergent evolution of  
614 defensin sequence, structure and function. *Cellular and molecular life sciences : CMLS*.  
615 2017;74(4):663-82.
  - 616 8. Shafee TM, Lay FT, Hulett MD, Anderson MA. The Defensins Consist of Two  
617 Independent, Convergent Protein Superfamilies. *Molecular biology and evolution*.  
618 2016;33(9):2345-56.
  - 619 9. Ganz T. Defensins: antimicrobial peptides of innate immunity. *Nature reviews*  
620 *Immunology*. 2003;3(9):710-20.
  - 621 10. Wimley WC, Selsted ME, White SH. Interactions between human defensins and  
622 lipid bilayers: evidence for formation of multimeric pores. *Protein science : a publication*  
623 *of the Protein Society*. 1994;3(9):1362-73.
  - 624 11. Brogden KA. Antimicrobial peptides: pore formers or metabolic inhibitors in  
625 bacteria? *Nature reviews Microbiology*. 2005;3(3):238-50.
  - 626 12. Yang D, Biragyn A, Kwak LW, Oppenheim JJ. Mammalian defensins in immunity:  
627 more than just microbicidal. *Trends in immunology*. 2002;23(6):291-6.
  - 628 13. Lehrer RI, Jung G, Ruchala P, Andre S, Gabius HJ, Lu W. Multivalent binding of  
629 carbohydrates by the human alpha-defensin, HD5. *Journal of immunology (Baltimore,*  
630 *Md : 1950)*. 2009;183(1):480-90.
  - 631 14. Chu H, Pazgier M, Jung G, Nuccio SP, Castillo PA, de Jong MF, et al. Human  
632 alpha-defensin 6 promotes mucosal innate immunity through self-assembled peptide  
633 nanonets. *Science (New York, NY)*. 2012;337(6093):477-81.
  - 634 15. Gwyer Findlay E, Currie SM, Davidson DJ. Cationic host defence peptides:  
635 potential as antiviral therapeutics. *BioDrugs : clinical immunotherapeutics,*  
636 *biopharmaceuticals and gene therapy*. 2013;27(5):479-93.
  - 637 16. Park MS, Kim JI, Lee I, Park S, Bae JY, Park MS. Towards the Application of  
638 Human Defensins as Antivirals. *Biomolecules & therapeutics*. 2018.
  - 639 17. Daher KA, Selsted ME, Lehrer RI. Direct inactivation of viruses by human  
640 granulocyte defensins. *Journal of virology*. 1986;60(3):1068-74.

- 641 18. Hazrati E, Galen B, Lu W, Wang W, Ouyang Y, Keller MJ, et al. Human alpha-  
642 and beta-defensins block multiple steps in herpes simplex virus infection. *Journal of*  
643 *immunology* (Baltimore, Md : 1950). 2006;177(12):8658-66.
- 644 19. Nakashima H, Yamamoto N, Masuda M, Fujii N. Defensins inhibit HIV replication  
645 in vitro. *AIDS* (London, England). 1993;7(8):1129.
- 646 20. Furci L, Sironi F, Tolazzi M, Vassena L, Lusso P. Alpha-defensins block the early  
647 steps of HIV-1 infection: interference with the binding of gp120 to CD4. *Blood*.  
648 2007;109(7):2928-35.
- 649 21. Demirkhanyan LH, Marin M, Padilla-Parra S, Zhan C, Miyauchi K, Jean-Baptiste  
650 M, et al. Multifaceted mechanisms of HIV-1 entry inhibition by human alpha-defensin.  
651 *The Journal of biological chemistry*. 2012;287(34):28821-38.
- 652 22. Ehmann D, Wendler J, Koeninger L, Larsen IS, Klag T, Berger J, et al. Paneth  
653 cell alpha-defensins HD-5 and HD-6 display differential degradation into active  
654 antimicrobial fragments. *Proceedings of the National Academy of Sciences of the United*  
655 *States of America*. 2019;116(9):3746-51.
- 656 23. Wroblewska Z, Wellish MC, Wolinsky JS, Gilden D. Comparison of human  
657 cytomegalovirus growth in MRC-5 human fibroblasts, brain, and choroid plexus cells in  
658 vitro. *J Med Virol*. 1981;8(4):245-56.
- 659 24. Berridge MV, Tan AS. Characterization of the cellular reduction of 3-(4,5-  
660 dimethylthiazol-2-yl)-2,5-diphenyltetrazolium bromide (MTT): subcellular localization,  
661 substrate dependence, and involvement of mitochondrial electron transport in MTT  
662 reduction. *Archives of biochemistry and biophysics*. 1993;303(2):474-82.
- 663 25. Ke N, Wang X, Xu X, Abassi YA. The xCELLigence system for real-time and  
664 label-free monitoring of cell viability. *Methods Mol Biol*. 2011;740:33-43.
- 665 26. Sinzger C, Grefte A, Plachter B, Gouw AS, The TH, Jahn G. Fibroblasts, epithelial  
666 cells, endothelial cells and smooth muscle cells are major targets of human  
667 cytomegalovirus infection in lung and gastrointestinal tissues. *The Journal of general*  
668 *virology*. 1995;76 ( Pt 4):741-50.
- 669 27. Sinzger C, Digel M, Jahn G. Cytomegalovirus cell tropism. *Current topics in*  
670 *microbiology and immunology*. 2008;325:63-83.
- 671 28. He JH, Gao JM, Huang CJ, Li CQ. Zebrafish models for assessing developmental  
672 and reproductive toxicity. *Neurotoxicol Teratol*. 2014;42:35-42.
- 673 29. Ball JS, Stedman DB, Hillegeass JM, Zhang CX, Panzica-Kelly J, Coburn A, et al.  
674 Fishing for teratogens: a consortium effort for a harmonized zebrafish developmental  
675 toxicology assay. *Toxicol Sci*. 2014;139(1):210-9.
- 676 30. Wang A, Chen F, Wang Y, Shen M, Xu Y, Hu J, et al. Enhancement of antiviral  
677 activity of human alpha-defensin 5 against herpes simplex virus 2 by arginine  
678 mutagenesis at adaptive evolution sites. *Journal of virology*. 2013;87(5):2835-45.
- 679 31. Jarczack J, Kosciuczuk EM, Lisowski P, Strzalkowska N, Jozwik A, Horbanczuk J,  
680 et al. Defensins: natural component of human innate immunity. *Human immunology*.  
681 2013;74(9):1069-79.
- 682 32. Lamiable A, Thevenet P, Rey J, Vavrusa M, Derreumaux P, Tuffery P. PEP-  
683 FOLD3: faster de novo structure prediction for linear peptides in solution and in complex.  
684 *Nucleic Acids Res*. 2016;44(W1):W449-54.
- 685 33. Sampaio KL, Jahn G, Sinzger C. Applications for a dual fluorescent human  
686 cytomegalovirus in the analysis of viral entry. *Methods Mol Biol*. 2013;1064:201-9.
- 687 34. Wilson SS, Wiens ME, Smith JG. Antiviral mechanisms of human defensins.  
688 *Journal of molecular biology*. 2013;425(24):4965-80.

- 689 35. Businger R, Deutschmann J, Gruska I, Milbradt J, Wiebusch L, Gramberg T, et al.  
690 Human cytomegalovirus overcomes SAMHD1 restriction in macrophages via pUL97.  
691 Nat Microbiol. 2019.
- 692 36. Muller P, Rogers KW, Jordan BM, Lee JS, Robson D, Ramanathan S, et al.  
693 Differential diffusivity of Nodal and Lefty underlies a reaction-diffusion patterning system.  
694 Science (New York, NY). 2012;336(6082):721-4.
- 695 37. Lee W, Tonelli M, Markley JL. NMRFAM-SPARKY: enhanced software for  
696 biomolecular NMR spectroscopy. Bioinformatics. 2015;31(8):1325-7.
- 697 38. Xia Y, Legge G, Jun KY, Qi Y, Lee H, Gao X. IP-COSY, a totally in-phase and  
698 sensitive COSY experiment. Magn Reson Chem. 2005;43(5):372-9.
- 699 39. Wommack AJ, Robson SA, Wanniarachchi YA, Wan A, Turner CJ, Wagner G, et  
700 al. NMR solution structure and condition-dependent oligomerization of the antimicrobial  
701 peptide human defensin 5. Biochemistry. 2012;51(48):9624-37.  
702  
703  
704  
705  
706  
707  
708  
709  
710  
711  
712  
713  
714  
715  
716  
717  
718  
719

720 **FIGURES**

**A**

Position: 1 2 3 4 5 6 7 8 9 10 11 12 13 14 15 16 17 18 19 20 21 22 23 24 25 26 27 28 29 30 31 32 33

1-33 (HNP4) **V C S C R L V F C R R T E L R V G N C L I G G V S F T Y C C T R V**

1-11 **V C S C R L V F C R R**

1-11 mod Ac-**v c s c r l v f c r r**-NH<sub>2</sub>

**B**

Position: 1 2 3 4 5 6 7 8 9 10 11 12 13 14 15 16 17 18 19 20 21 22 23 24 25 26 27 28 29 30 31 32

1-32 (HD5) **A T C Y C R T G R C A T R E S L S G V C E I S G R L Y R L C C R**

1-9 **A T C Y C R T G R**

1-9 mod Ac-**a t c y c r t G r**-NH<sub>2</sub>

1-13 **A T C Y C R T G R C A T R**

1-28 **A T C Y C R T G R C A T R E S L S G V C E I S G R L Y R**

7-32 **T G R C A T R E S L S G V C E I S G R L Y R L C C R**

10-27 **C A T R E S L S G V C E I S G R L Y**

10-32 **C A T R E S L S G V C E I S G R L Y R L C C R**

26-32 **L Y R L C C R**

721

722

723 **Figure 1: Primary amino acid sequence alignment of HNP4, HD5 and all**

724 **corresponding fragments. (A) HNP4 or (B) HD5 full length proteins are highlighted in**

725 **red. D-amino acids appear in lower case letters.**

726

727

728

729

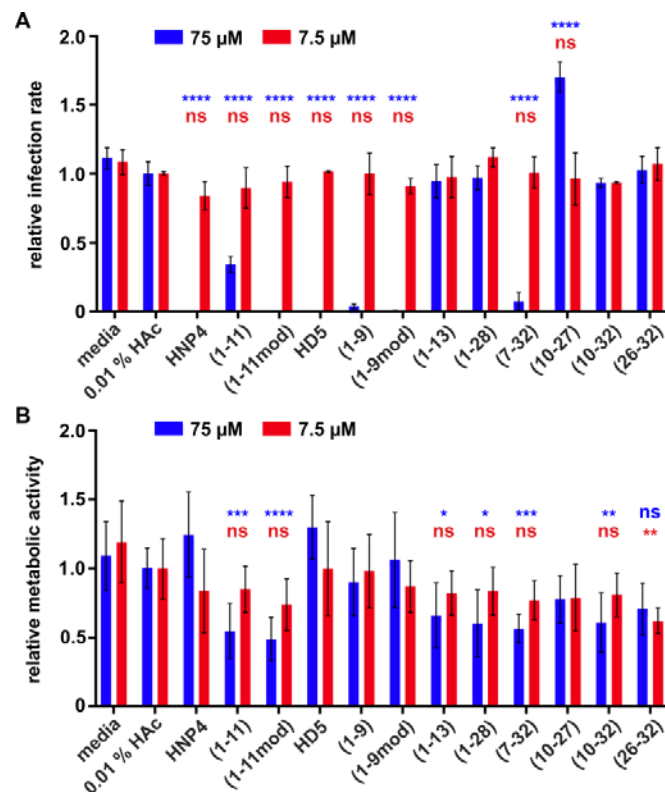
730

731

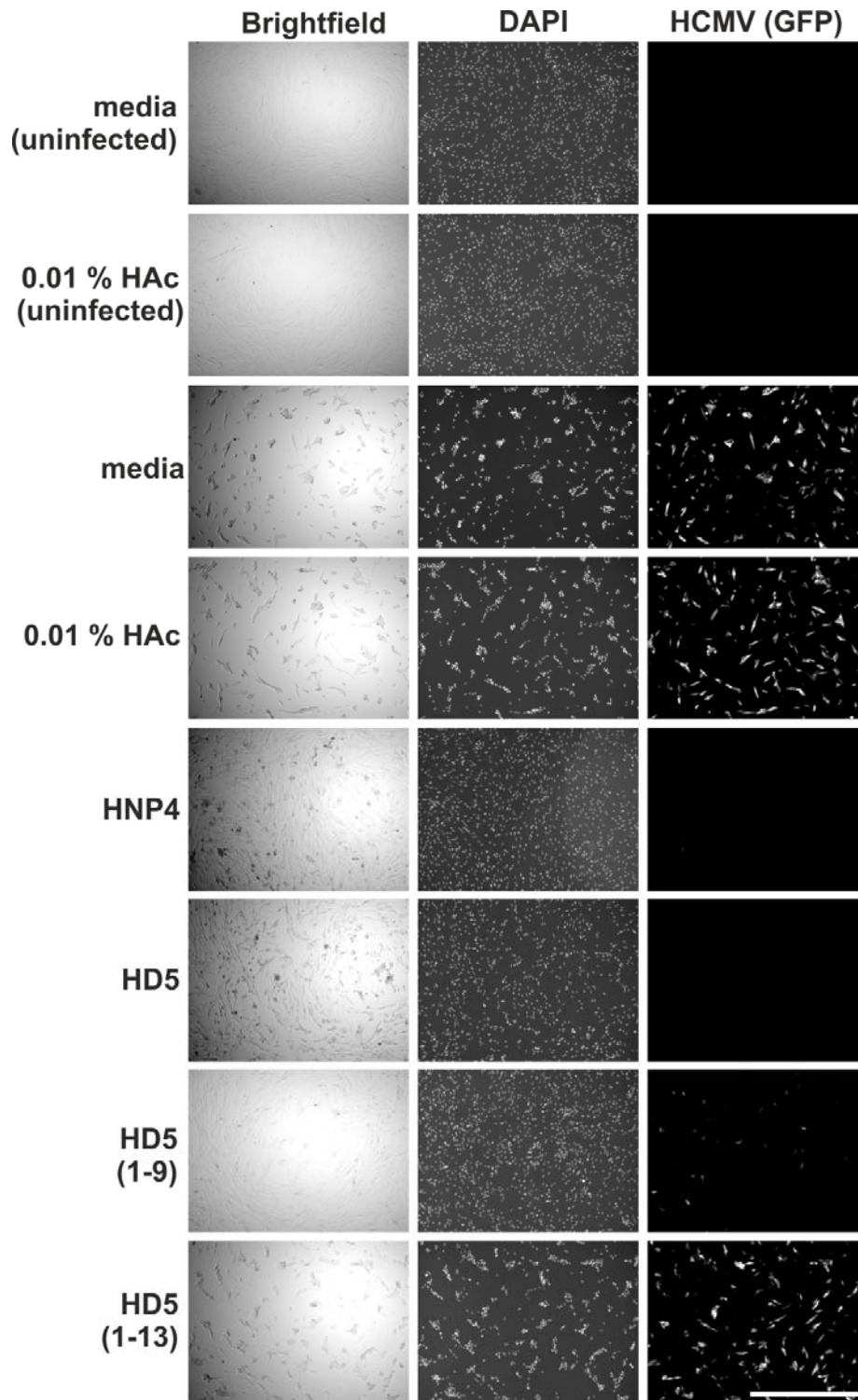
732

733

734



735 **Figure 2: Antiviral activity and cytotoxicity of  $\alpha$ -defensin-derived peptides. (A)** HFF  
736 were infected with TB40/E- $\Delta$ UL16-eGFP (MOI of 0.5) and treated with the indicated  
737 peptides in concentrations of 7.5  $\mu$ M and 75  $\mu$ M. After 40 h of incubation cells were  
738 fixed, nuclei stained with DAPI and infection rates measured by imaging with a  
739 microplate imager and automated counting of DAPI+ and GFP+ cells. The graph shows  
740 the calculated relative infection rate (GFP+/DAPI+, normalized to 0.01 % HAc) **(B)** HFF  
741 were treated with the indicated peptides in concentrations of 7.5  $\mu$ M and 75  $\mu$ M. After 40  
742 h incubation metabolic activity of cells was measured by MTT. The graph shows the  
743 relative metabolic activity (absorption at 570 nm, normalized to 0.01 % HAc). For (A) and  
744 (B): both graphs show mean  $\pm$  SD from triplicate measurements of three independent  
745 experiments). ns, not significant; \*\*\*\*,  $p < 0.0001$ ; \*\*\*,  $p < 0.001$ ; \*\*,  $p < 0.01$ ; \*,  $p < 0.05$ .  
746 Statistical test used: ordinary one-way-ANOVA with multiple comparisons with Dunnett  
747 correction.

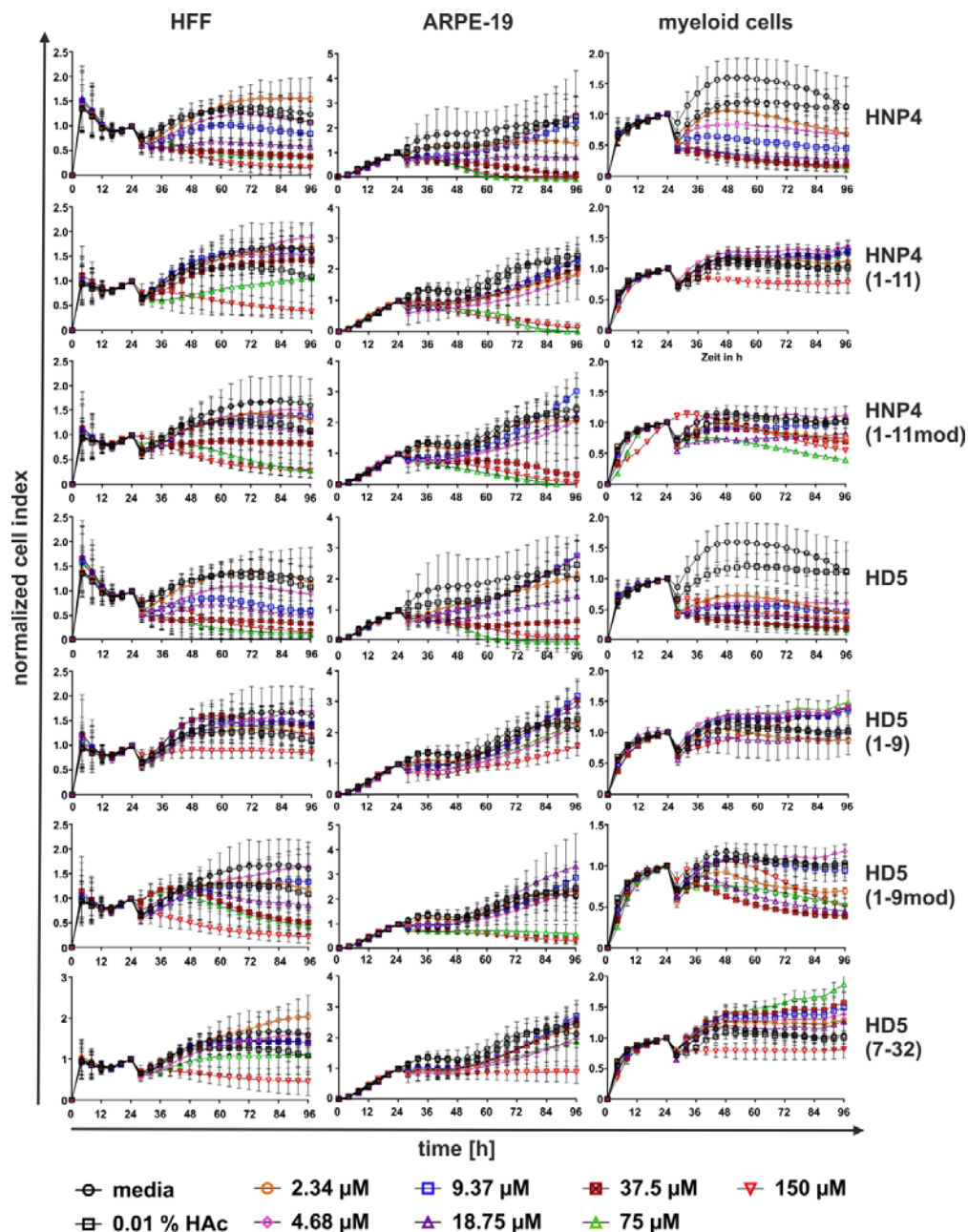


748

749 **Figure 3: Suppression of HCMV infection and cytopathic effects by  $\alpha$ -defensin-**

750 **derived peptides.** Representative images of HFF cells treated with 75  $\mu$ M of peptide as

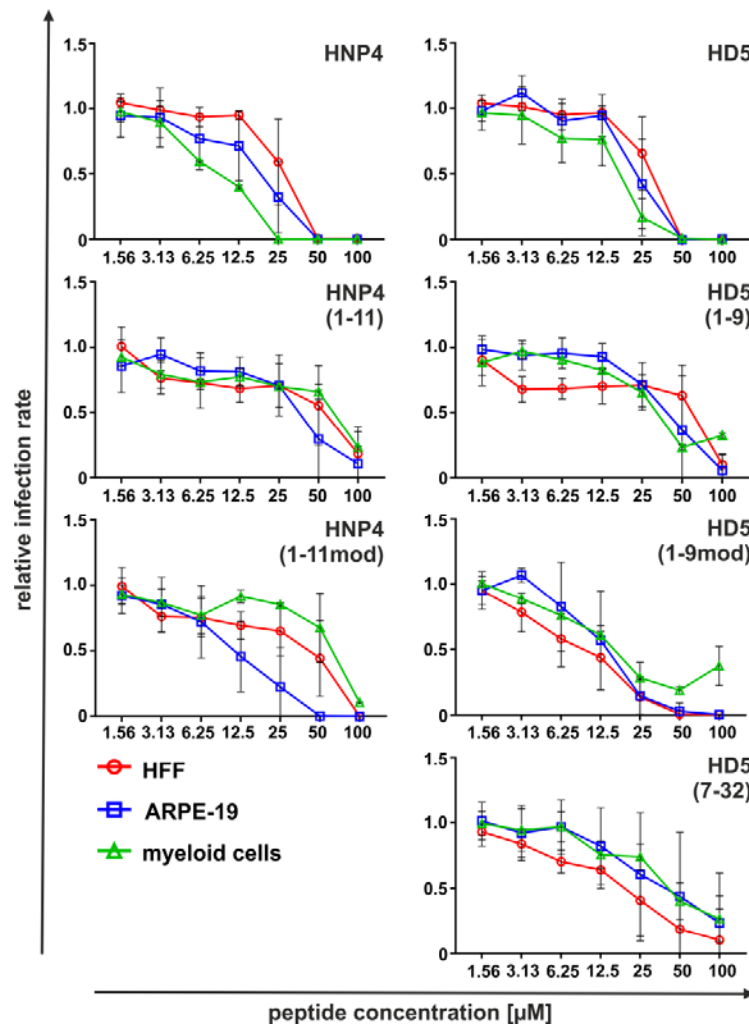
751 detailed in Fig. 2A. The scale bar indicates 1000  $\mu$ m.



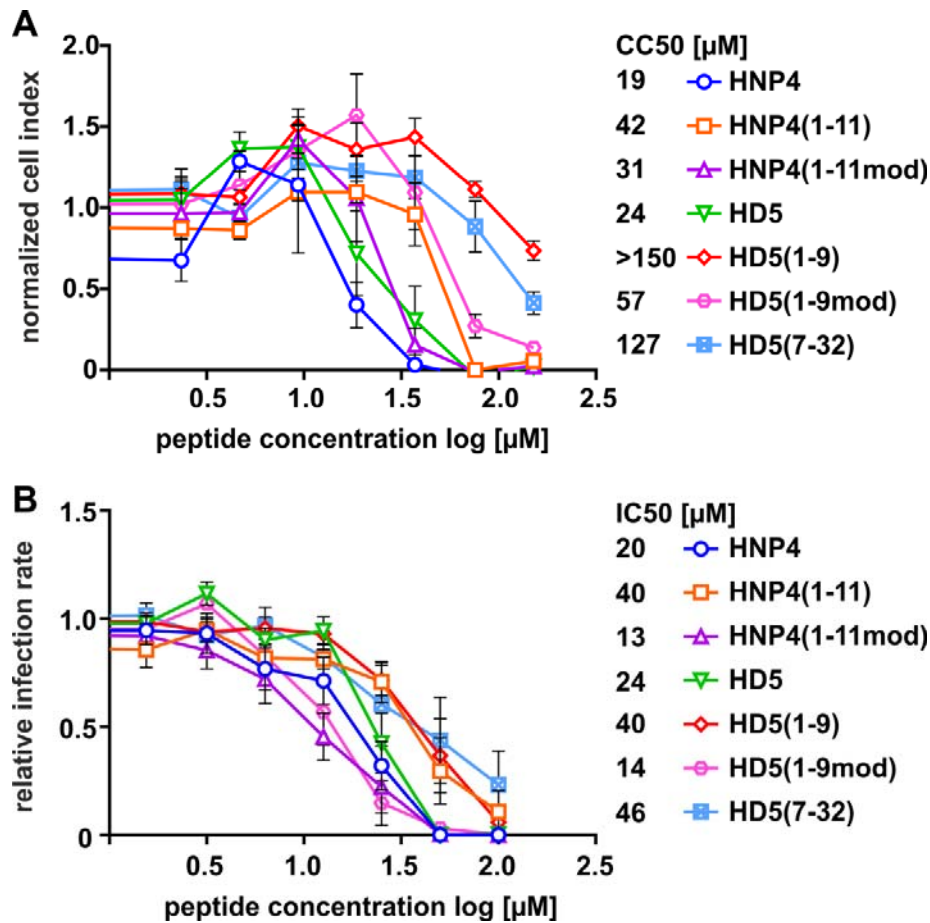
752

753 **Figure 4: Impact of  $\alpha$ -defensin-derived peptides on cellular attachment and**  
 754 **growth.** HFF, ARPE-19 and macrophages were treated 24 h post seeding with the  
 755 indicated concentrations of the different peptides. Measurement of electrical impedance  
 756 was done every 30 min over 72 h (normalized to 24 h value, mean  $\pm$  SD from duplicates  
 757 of three independent measurements for HFF and ARPE-19 and one to three  
 758 independent measurements for macrophages).





759 **Figure 5: Dose-dependent inhibition of HCMV-infection by  $\alpha$ -defensin-derived**  
760 **peptides.** HFF, ARPE-19 and PMA-differentiated THP-1 cells or macrophages were  
761 infected with HCMV TB40/E- $\Delta$ UL16-EGFP and treated with the various peptides in  
762 different concentrations. After 40 h incubation, cells were fixed and HCMV-infected cells  
763 identified by IE1/2 antigen staining (in addition to GFP staining we used IE1/2 for higher  
764 sensitivity as compared to the experiment shown in Fig. 1). Nuclear staining was done  
765 with DAPI. Infection rates were measured by imaging with a microplate imager and  
766 automated counting of DAPI+ and IE1/2+ cells. The calculated infection rate for all three  
767 cell types is shown (IE1/2+/DAPI+, normalized to medium only, mean  $\pm$  SD from  
768 duplicate infections of three independent experiments for HFF and ARPE-19 and one  
769 experiment for THP-1/macrophages).



770

771 **Figure 6: Calculation of IC50 and CC50 for  $\alpha$ -defensin-derived peptides. (A) CC50**

772 was determined by measuring electrical impedance of ARPE-19 cells at 72 h post

773 incubation (96 h total time) with different concentrations of the respective peptides

774 (compare Fig. 4). (B) IC50 was determined by measuring HCMV infection of ARPE-19

775 cells post incubation with different concentrations of the respective peptides (compare

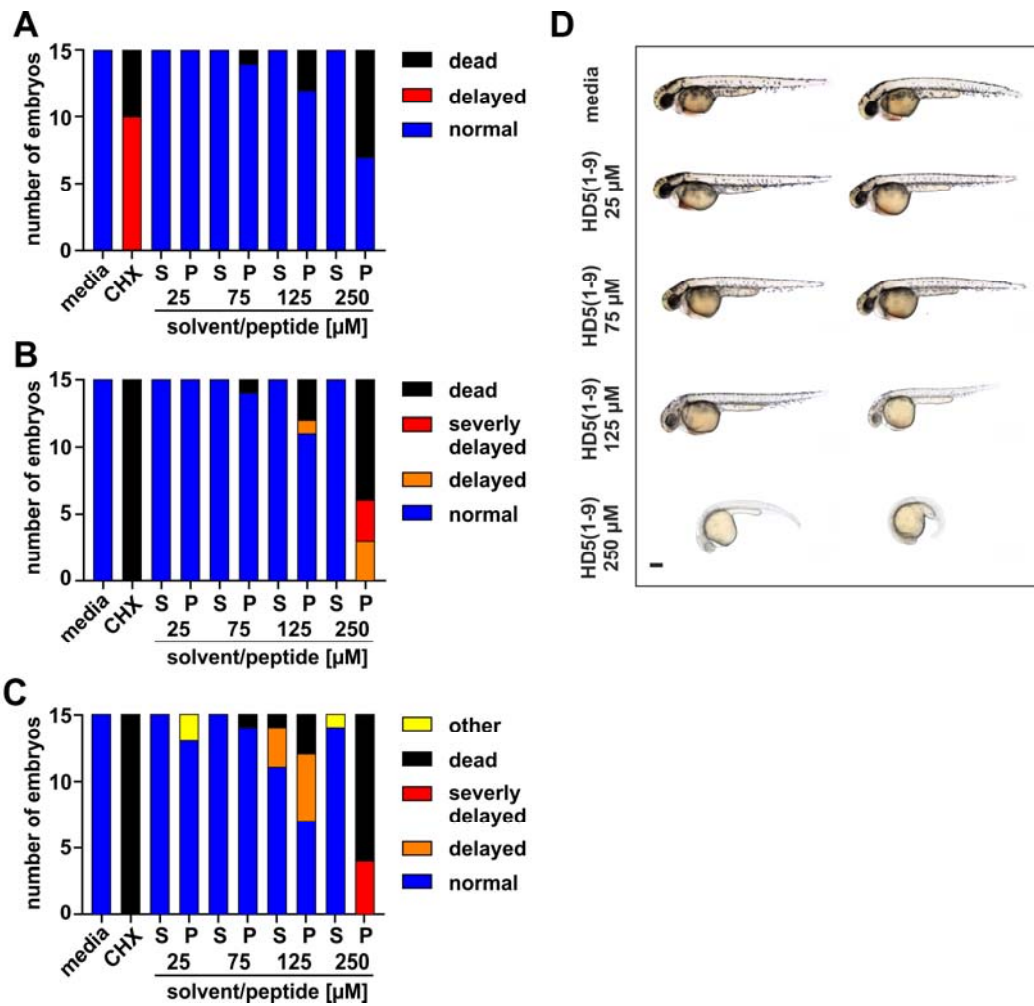
776 Fig. 4). Mean  $\pm$  SEM from three independent experiments with duplicate infections.

777

778

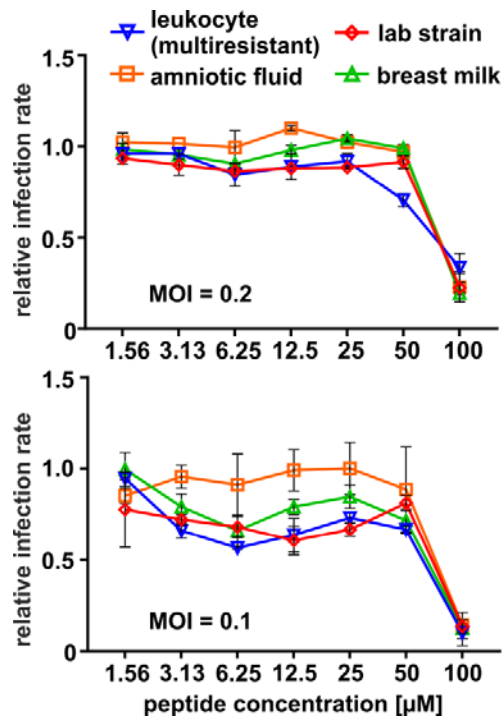
779

780



781  
782 **Figure 7: Impact of HD5(1-9) on embryonic development of zebrafish.** 6-7 h post-  
783 fertilization (hpf), peptides at different concentrations were added to the embryos. At 13  
784 hpf (A), 24 hpf (B) and 48 hpf (C) the embryos were visually inspected. Solvent: PBS,  
785 CHX: cycloheximide. (D) Representative images of phenotypes at 48 hpf are shown.  
786 The scale bar indicates 250 μM.

787  
788  
789  
790



791

792 **Figure 8: HD5(1-9) inhibits infection with primary patient-derived HCMV isolates.**

793 HFF were infected with different clinical HCMV isolates and TB40/E-ΔUL16-eGFP as  
794 reference strain with an MOI of 0.2 or 0.1 and treated with HD5(1-9) in different  
795 concentrations. After 40 h incubation, cells were fixed and HCMV-infected cells identified  
796 by IE1/2 antigen staining. Nuclear staining was done with DAPI. Infection rates were  
797 measured by imaging with a microplate imager and automated counting of DAPI+ and  
798 IE1/2+ cells. The graphs show the calculated infection rate (IE1/2+/DAPI+, normalized to  
799 medium only, mean ± SD from duplicate infections each).

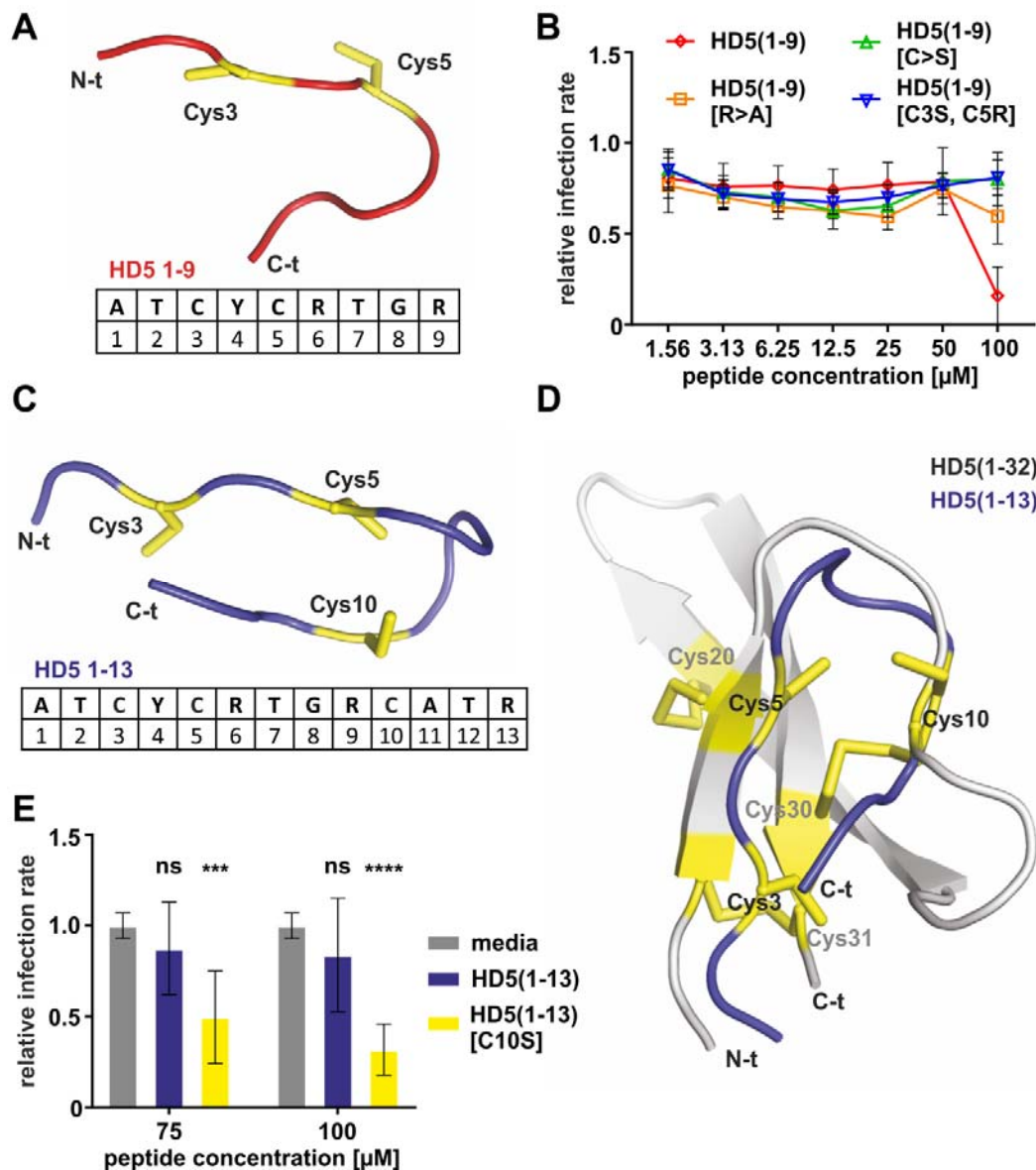
800

801

802

803

804



805

806 **Figure 9: Cysteine and arginine residues in HD5(1-9) mediate its antiviral activity.**

807 **(A)** Model and aa-sequence of HD5(1-9); structural model generated by PEP-FOLD 3

808 **(32).** **(B)** HFF were infected with TB40/E-ΔUL16-eGFP (MOI of 0.2) and treated with the

809 indicated derivatives of the peptide fragment HD5(1-9) in different concentrations. After

810 40 h incubation, cells were fixed and HCMV-infected cells identified by IE1/2 antigen

811 staining. Nuclear staining was done with DAPI. Infection rates were measured by

812 imaging with a microplate imager and automated counting of DAPI+ and IE1/2+ cells.

813 The graphs show the calculated infection rate (IE1/2+/DAPI+, normalized to medium  
814 only, mean  $\pm$  SD from duplicate infections of three independent experiments). **(C)** Model  
815 and aa-sequence of HD5(1-13); structural model generated by PEP-FOLD 3. **(D)**  
816 Structural alignment of HD5(1-32) crystal structure (39) (pdb: 2lxz) (grey), and prediction  
817 model of peptide HD5(1-13) generated by PEP FOLD 3 (blue). Cys are marked in yellow  
818 and arrows represent  $\beta$ -strands. Alignment generated with PyMol. **(E)** Similar  
819 experimental setup as in (B), however HD5(1-13) and HD5(1-13)[C10S] with a mutated  
820 cysteine at position ten to serine were used (mean  $\pm$  SD from duplicate infections of  
821 three independent experiments). ns, not significant; \*\*\*\*,  $p < 0.0001$ ; \*\*\*,  $p < 0.001$ .  
822 Statistical test used: ordinary one-way-ANOVA with multiple comparisons with Dunnett  
823 correction.

824

825

826

827

828

829

830

831

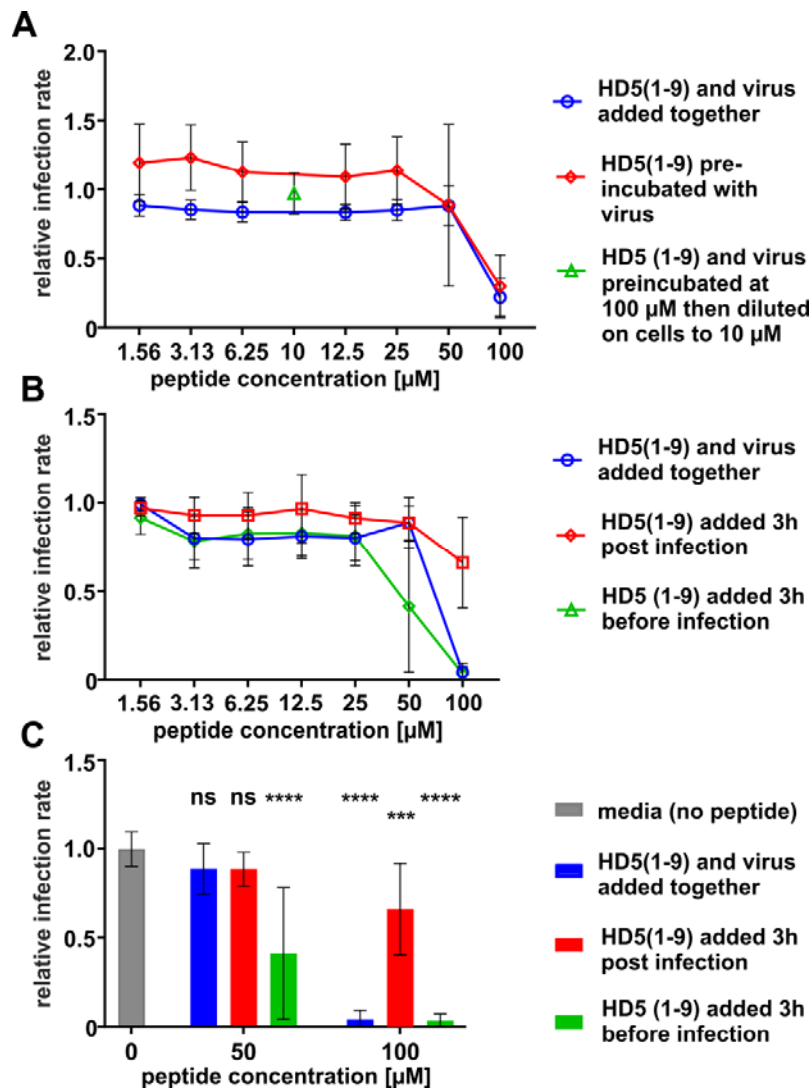
832

833

834

835

836



837

838 **Figure 10: HD5(1-9) inhibits an early step during HCMV entry.** (A) HFF were infected  
 839 with TB40/E- $\Delta$ UL16-eGFP at a MOI of 0.2. HD5(1-9) was either given directly to the  
 840 cells together with the viral inoculum or pre-incubated for 1 h at 37 °C with the virus  
 841 preparation and then added to the cells. In one condition, HD5(1-9) and the virus  
 842 preparation were pre-incubated at a concentration of 100  $\mu\text{M}$  and diluted ten-fold on the  
 843 cells to a final HD5(1-9) concentration of 10  $\mu\text{M}$ . After 40 h incubation, cells were fixed  
 844 and HCMV-infected cells identified by IE1/2 antigen staining. Nuclear staining was done  
 845 with DAPI. Infection rates were measured by imaging with a microplate imager and

846 automated counting of DAPI+ and IE1/2+ cells. The graph shows the calculated infection  
847 rate (IE1/2+/DAPI+, normalized to medium only, mean  $\pm$  SD from duplicate infections of  
848 three independent experiments). **(B)** Similar infection protocol as in (A) however we  
849 tested two conditions in which HD5(1-9) was given to the cells either 3 hours before, or  
850 alternatively 3 hours post infection with TB40/E- $\Delta$ UL16-eGFP. The graph shows the  
851 calculated infection rate (IE1/2+/DAPI+, normalized to medium only, mean  $\pm$  SD from  
852 duplicate infections of three independent experiments). **(C)** Statistical analysis of the  
853 data depicted in (B) for concentrations of 50  $\mu$ M and 100  $\mu$ M peptide. ns, not significant;  
854 \*\*\*\*,  $p < 0.0001$ ; \*\*\*,  $p < 0.001$ . Statistical test used: ordinary one-way-ANOVA with  
855 multiple comparisons with Dunnett correction.

856

857

858

859

860

861

862

863

864

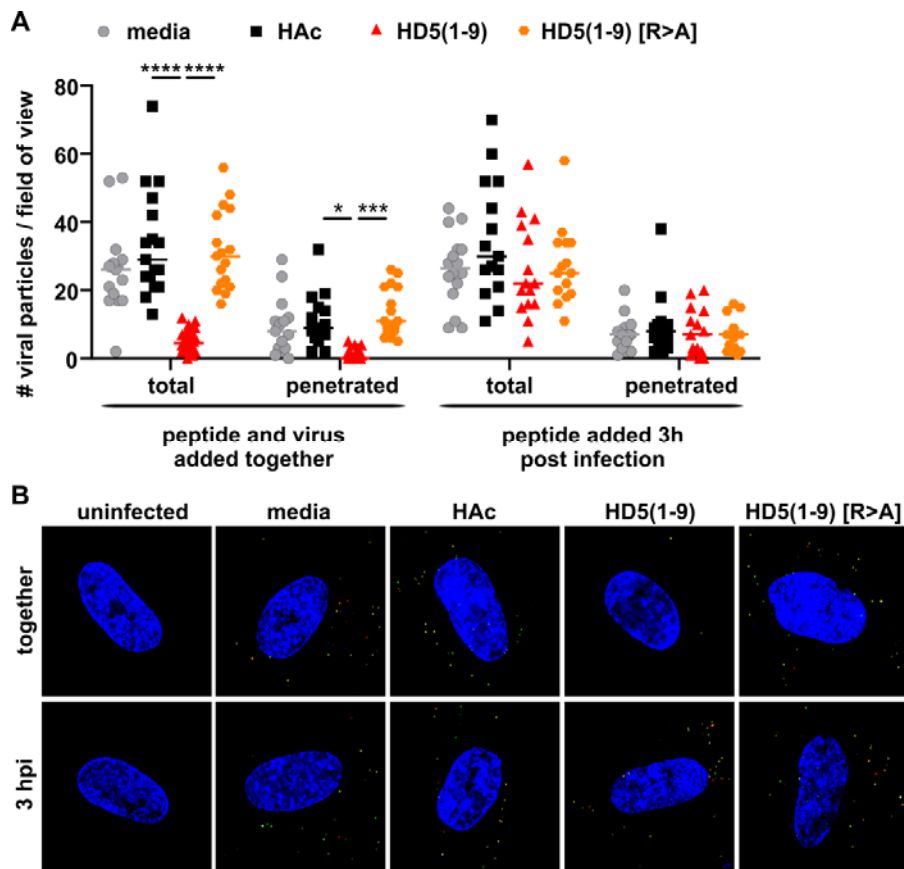
865

866

867

868





869 **Figure 11: HD5(1-9) inhibits cellular attachment of HCMV particles.** HFF were  
870 infected at an MOI of 2 with the dual fluorescent virus TB40-BAC<sub>KL</sub>-UL32eGFP-  
871 UL100mCherry, expressing pp150 (pUL32) fused to eGFP and gM (pUL100) fused to  
872 mCherry. This allows to discriminate enveloped virus particles (eGFP+/mCherry+), from  
873 penetrated viruses (eGFP+). HD5(1-9) or HD5(1-9) [R>A] were added either  
874 simultaneously with the virus or 3 hpi at a final concentration of 100  $\mu$ M. 6 h later cells  
875 were fixed and DNA stained and subjected to fluorescence microscopy. (A) For each  
876 condition, the total number of cell-associated viral particles or penetrated particles was  
877 counted for at least 15 cells. Statistical test used: ordinary one-way-ANOVA with multiple  
878 comparisons with Dunnett correction; \*\*\*\*,  $p < 0.0001$ ; \*\*\*,  $p < 0.001$ ; \*,  $p < 0.05$ . (B)  
879 Representative images of the different conditions quantified in (A). The result was  
880 confirmed in an additional independent experiment.